IEEE Access
Multidisciplinary | Rapid Review | Open Access Journal

Received February 21, 2020, accepted March 10, 2020, date of publication March 18, 2020, date of current version March 27, 2020.

Digital Object Identifier 10.1109/ACCESS.2020.2981658

Integrated Variable Speed Limits and Lane-Changing Control for Freeway Lane-Drop Bottlenecks

YUQING GUO[1], HUILE XU[1], YI ZHANG[1,2,3], (Member, IEEE), AND DANYA YAO[1,2], (Member, IEEE)

[1]Department of Automation, Tsinghua University, Beijing 100084, China
[2]Jiangsu Province Collaborative Innovation Center of Modern Urban Traffic Technologies, Nanjing 210096, China
[3]Tsinghua-Berkeley Shenzhen Institute (TBSI), Shenzhen 518055, China

Corresponding author: Danya Yao (yaody@tsinghua.edu.cn)

This work was supported in part by the National Key Research and Development Program of China under Grant 2017YFB0102601, and in part by the National Natural Science Foundation of China under Grant 61673233.

ABSTRACT There are generally two kinds of traffic control strategies to relieve traffic congestion in lane-drop bottlenecks: variable speed limits (VSL) control and lane-changing (LC) control. However, VSL has limited or even no effect due to many mandatory LC maneuvers near bottlenecks, while LC fails to reduce traffic congestion when traffic demand is high. Although a few control methods combine VSL and LC, they do not consider the interaction between VSL and LC, which rules out many potentially good alternatives. We instead propose an integrated VSL and LC control method under a connected and automated vehicle (CAV) environment, which can consider the interaction and simultaneously find the values of LC numbers and speed limits to maximize traffic efficiency. Our control is in the framework of the model predictive control (MPC), which consists of prediction, optimization, and implementation. We adopt an improved multi-class cell transmission model (CTM) for traffic state prediction, then use the genetic algorithm (GA) for optimization which optimizes traffic network performance, and implement our control method in the SUMO platform. Simulation results demonstrate that our control method greatly improves the capacity of the road and is robust to different traffic demands and scenarios. Our control outperforms no control and VSL-only control in travel time and exhaust emissions, which reduces total travel time by 23.86% to 44.62% and exhaust emissions by 10.29% to 48.19%.

INDEX TERMS Connected and automated vehicles (CAVs), lane-changing (LC) control, lane-drop bottlenecks, variable speed limits (VSL).

I. INTRODUCTION

Lane-drop (reduction in the number of lanes), such as incident lane blockage, road construction, or inherent design flaws, is common in freeways due to various reasons. Lane drops cause local traffic disruptions on a freeway and will be active bottlenecks when the traffic demand is high [1]. Once the congestion occurs at these bottlenecks, the capacity will be lower than the capacity before the congestion, causing the so-called ''capacity drop'' phenomenon [2].

The main reason for this is the concentrated mandatory lane-changing (LC) maneuvers near bottlenecks as Fig. 1 shows. These LC maneuvers increase mutual influences between vehicles, leading to more acceleration and deceleration maneuvers of vehicles near bottlenecks, which can cause traffic congestion, and even reduce traffic safety [2], [3]. It is, therefore, necessary to take measures to control traffic to improve traffic efficiency near bottlenecks.

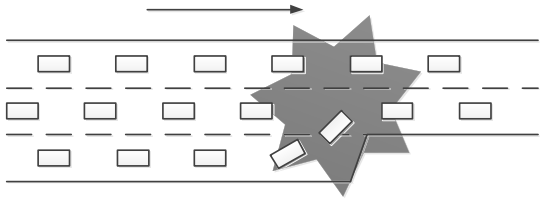

FIGURE 1. Mandatory LC maneuvers near a lane-drop bottleneck.

An intuitive idea is to reduce traffic density and the inflow entering bottlenecks by limiting speed, which can reduce mutual influences between vehicles. Therefore, a lot

The associate editor coordinating the review of this manuscript and approving it for publication was Arun Prakash.

of existing work adopts variable speed limits (VSL) control methods to overcome the ''capacity drop'' phenomenon [4] and improve traffic efficiency near lane-drop bottlenecks [5], [6]. By limiting upstream speed, they starve the inflow to the bottleneck and reduce traffic density, which reduces traffic congestion caused by LC near bottlenecks [7].

However, the state-of-art studies find that mandatory LC behaviors near bottlenecks may result in unsatisfactory effects of these VSL methods [8], [9]. Zhang and Ioannou [10] indicated that most existing VSL methods have little improvement in microscopic simulations in terms of traffic mobility. Besides, in some cases, the speed limit values generated by the VSL control may be small and sometimes even less than 20 km/h, which is not allowed on the freeways in practice.

As mandatory LC near bottlenecks is the main reason for the capacity drop, researchers adopt LC advisory as in [2] to encourage LC at proper locations to mitigate the negative effects of mandatory LC near lane-drop bottlenecks. They decrease the chance of traffic breakdown by optimizing vehicle distribution in lanes. However, when the traffic demand is high, only using LC control is not enough for reducing traffic congestion [11].

Recent work illustrates the necessity to combine VSL and LC control strategies and proposes combined control methods [10]. To the best of our knowledge, Zhang *et al.* are the first to combine VSL and LC control to provide LC recommendations to vehicles upstream of bottlenecks [11]. Existing work uses LC control to improve road capacity of bottlenecks and then adopts VSL to reduce traffic congestion when the traffic demand is higher than the road capacity. However, without consideration of the interaction between VSL and LC control, existing work loses many potentially good alternatives, which makes the combined VSL and LC control unable to fully exert control effects to reduce the traffic congestion, especially under high traffic demands.

We instead propose an integrated VSL and LC control method, which fully considers the mutual influence between VSL and LC control. Different from existing methods, which first use LC to improve road capacity and then use VSL to reduce congestion, we simultaneously find the values of LC numbers and speed limits to maximize traffic efficiency. In this way, our method can benefit from the two control strategies fully.

To achieve individual control over each vehicle, our work needs the help of connected and automated vehicles (CAVs). With the development of vehicle-to-everything (V2X) and automated driving technology, CAVs can help us not only obtain the whole spatiotemporal traffic information, but also send information to each CAV and advise CAVs to change state at different locations [12], [13].

To reduce computational complexity, we divide the freeway upstream a bottleneck into several cells by length and into sub-cells further by lanes and assume that vehicles in the same sub-cell have the same speed limit. The control problem is to find the optimal combination of control measures that results in the best network performance. Our control variables are speed limits in different sub-cells and LC numbers of vehicles in different cells. This helps us make full use of the efficiency of the road by applying different speed limits to different lanes and consider the mutual influence between VSL and LC.

To find the optimal combination of control variables, we apply a model predictive control (MPC) framework. MPC includes three parts: an internal dynamic model for prediction, an optimization process minimizing a cost function over a receding horizon, and implementation of the control strategy solved by the optimization process [5].

Our control method is carried out on an open-source microscopic traffic simulation platform, SUMO. In SUMO, traffic data (including traffic density, speed, and flow) at the current time interval are collected with the help of V2X. Based on the collected traffic data, an improved multi-class cell transmission model (CTM) is used to predict traffic state during the receding horizon. We adopt the multi-class CTM proposed by Yu and An [14], for it can more truly reflect the heterogeneous nature of real traffic networks. However, it does not consider LC, so we improve it by considering LC control between different sub-cells to predict the density, speed, and flow rate in each sub-cell better.

Based on the dynamic traffic model, a cost function over a receding horizon can be computed with respect to different speed limits and LC vehicle numbers. We try to minimize travel time and maximize travel distance by calculating total time spent (TTS) and total travel distance (TTD) in the cost function. Considering the non-convexity of the cost function, the genetic algorithm (GA) is adopted to find the optimal speed limits and LC vehicle numbers over the receding horizon in the optimization process. The calculation of the optimization process is solved in python and sent to SUMO through the SUMO traffic control interface (TraCI). Then CAVs change their states in a control horizon according to the received speed limits and LC vehicle numbers. At the next starting time of a control horizon, the procedure of prediction, optimization, and implementation is repeated. To validate the effectiveness of our control method, some simulation experiments are carried out. Simulation results show that our new refined integrated VSL and LC control outperforms no control and VSL-only control.

The rest of this paper is structured as follows. Section II introduces the background and Section III introduces the multi-class CTM and our extensions for traffic state prediction. A combined VSL and LC control method is proposed in Section IV to maximize future traffic efficiency. In Section V, SUMO simulation results under different traffic demands and incident scenarios are analyzed to verify the effectiveness and robustness of our method. Section VI presents the conclusions and scope for future research.

II. BACKGROUND

Road capacity drops sharply at lane-drop bottlenecks, especially in mixed flows containing trucks and other heavy

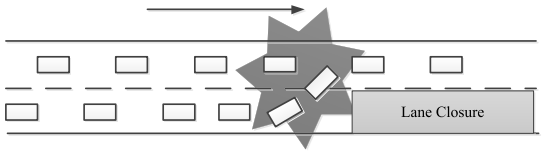

FIGURE 2. Freeway lane-drop bottleneck caused by lane closure.

vehicles. To clarify the capacity drop phenomenon and our approach clearly, we consider a two-lane freeway with a lane-drop bottleneck caused by lane closure and without on-ramps, off-ramps, and other bottlenecks as in Fig. 2. The lane closure can be caused by various reasons. This paper takes the lane closure caused by a car incident as an example, and lane closure caused by other reasons can be dealt with in a similar way. Assuming Q is the capacity of the two-lane freeway, when the road segment changes from two lanes to one lane, the ideal capacity of the bottleneck after the incident should be $Q_b = 1/2Q$. However, due to frequent LC, acceleration, and deceleration maneuvers, the capacity cannot reach $1/2Q$ and even drops significantly [2].

Existing control methods combined VSL and LC to solve the above problem. They use LC control to reduce LC behaviors at the bottleneck by reminding vehicles to change lanes in advance. Then, they try to reduce the interplay between vehicles by limiting their speeds, i.e., VSL control. They execute the LC control and VSL control successively without realizing that in the step of LC control, when traffic demand is high, some vehicles are unable to execute the LC control command due to the lack of sufficient gaps in the target lane. They suffer from the ignorance of the interaction between VSL and LC, which leads to a loss of many potentially good feasible combinations of VSL and LC. This makes existing work fail to maximize traffic efficiency.

To fill this gap, we propose a cell-based integrated VSL and LC control method. Unlike existing control methods, our method considers the interaction between VSL and LC in the formulas of multi-class CTM and finds the proper combination of VSL and LC by solving an optimization problem of online MPC. By doing so, an optimal combination of VSL and LC is solved through optimization to truly achieve the coordination control of VSL and LC.

Our control method is implemented with the help of CAVs. We assume that all vehicles in our work are CAVs. With V2X, it is possible to send information to each CAV and advise CAVs to change speed and make LC at different locations [15]. This offers the opportunity to distribute LC maneuvers at different places and smooth traffic flow.

III. TRAFFIC PREDICTION MODEL

To improve the stability of our control method, the desired coordination of speed limit values and LC numbers should maximize traffic efficiency in a given horizon. Accordingly, we develop online MPC for traffic control, for MPC can deal with multi-criteria optimization and take disturbances into account [5]. In MPC, an appropriate and accurate traffic prediction model is crucial.

Lighthill-Whitham-Richards (LWR) model, METANET model, and CTM are the three most popular models used for traffic prediction [16], [17]. However, these models neglect the differences among different kinds of vehicles. This may cause inaccurate prediction and lead to control failure for ignoring traffic heterogeneity, especially when traffic involves heavy vehicles [18]. The common approach considering multiple types of vehicles adopts a metric called Passenger Car Equivalent (PCE) by representing the influence of each vehicle in terms of the equivalent number of passengers per car [19], [20]. However, under different traffic conditions, the PCE is different. In consideration of dynamic and static characteristics of different vehicle types, Lint *et al.* [18] proposed the FASTLANE model by using dynamic PCEs (DPCES). Based on DPCEs, extended versions of multi-class METANET [21] and CTM [14] are proposed. These models mainly characterize mixed flows of cars and trucks. Later, mixed flow models consisting of Powered Two-Wheelers (PTWs) are also proposed [22]. This paper excludes PTWs according to the actual vehicle types on Chinese freeways.

Compared with other models, CTM is computationally tractable and easy for us to analyze the evolution of traffic flow under traffic control [23]. The multi-class CTM based on DPCEs is suitable for online MPC control [14]. However, it does not consider LC behaviors between different lanes. Some studies consider LC behaviors between different lanes and extend the CTM to multi-lane CTMs [24], [25]. However, these multi-lane CTMs do not consider different classes of vehicles. Pan *et al.* [26] proposed the multi-class multi-lane model for freeway traffic which focused on CAVs and regular human-piloted vehicles without considering the difference between passenger cars and heavy vehicles. Tiaprasert *et al.* [27] proposed a multi-class multi-lane CTM with first-in-first-out (FIFO) property to predict the traffic state when a fast vehicle (such as a car) cannot overtake a slow vehicle (such as a truck) due to the limitation of single-lane roads. The multi-lane CTM with FIFO property can improve the accuracy of traffic state estimation at the cost of computational complexity. To achieve a trade-off between the prediction accuracy and computational complexity, we therefore improve the multi-class CTM based on DPCEs in [14] to be a multi-class multi-lane CTM to make it more suitable for our integrated VSL and LC control. We refer to [14] for a full description of the multi-class CTM. For the sake of self-containedness, we repeat the original multi-class CTM here.

A. ORIGINAL MULTI-CLASS CTM

The original multi-class CTM proposed by Yu and An [14] is a multi-class version of the CTM. CTM is a discrete-time model and predicts macroscopic traffic behavior on a given freeway segment by dividing the freeway segment into homogeneous sections, i.e., cells. The CTM numbers these cells $i = 1, 2, \ldots, N$ starting downstream. The density of the cells at each time step is updated based on the conservation of inflows and outflows.

The main feature of the multi-class CTM is that it uses DPCEs to transform different vehicle classes into a representative vehicle class [14], [28]. DPCE considers dynamic and static characteristics of different vehicle types that involve physical characteristics, real-time speed and minimum headway of vehicles. In multi-class CTM, DPCE $\eta_{i,j}(k)$ for vehicle class j in cell i is as follows:

$$\eta_{i,j}(k) = \frac{sd_j + HW_j v_{i,j}(k)}{sd_{car} + HW_{car} v_{i,car}(k)}, \tag{1}$$

where k indicates the time instant $t = kT$, and T is the time step for the simulation of the traffic flow. sd_j is the gross stopping distance gap of vehicle type j, $v_{i,j}(k)$ is the average speed of vehicle type j in cell i during time interval k, and HW_j is the minimum headway of vehicle type j. Therefore, $sd_j + HW_j v_{i,j}(k)$ is the gross distance gap of vehicle type j. According to $\eta_{i,j}(k)$, when there are J types of vehicles, the equilibrium density $E\rho_i(k)$ on the ith cell during time interval k is [14]:

$$E\rho_i(k) = \sum_{j=1}^{J} \eta_{i,j}(k)\rho_{i,j}(k), \tag{2}$$

where $\rho_{i,j}(k)$ is the average density of vehicle type j in cell i during time interval k.

For the original multi-class CTM, the basic equations for computing flow and density of vehicle type j in cell i are:

$$q_{i,j}(k) = \rho_{i,j}(k) v_{i,j}(k), \tag{3}$$

$$\rho_{i,j}(k+1) = \rho_{i,j}(k) + \frac{T}{l}\left(q_j^{i-1,i}(k) - q_j^{i,i+1}(k)\right), \tag{4}$$

with $q_{i,j}(k)$ the flow of vehicle type j in cell i, $q_j^{i,i+1}(k)$ the flow of vehicle type j from cell i to cell $i+1$, and l the cell length.

To estimate $q_j^{i,i+1}(k)$ in (4), traffic demand of vehicle type j from cell i to cell $i+1$ is needed. Traffic demand transferring from cell i to cell $i+1$ needs to be distributed among different vehicle types and is proportional to the traffic composition on cell i [18]. The composition is represented by the flow ratio $P_{i,j}(k)$ of vehicle type j in cell i during time interval k. The traffic composition $P_{i,j}(k)$ can be calculated as [14]:

$$P_{i,j}(k) = \frac{\eta_{i,j}(k) v_{i,j}(k) \rho_{i,j}(k)}{\sum_{j=1}^{J} \eta_{i,j}(k) v_{i,j}(k) \rho_{i,j}(k)}. \tag{5}$$

So the flow $q_j^{i,i+1}(k)$ of vehicle type j from cell i to $i+1$ can be calculated as [14]:

$$q_j^{i,i+1}(k) = \frac{1}{\eta_{i,j}(k)} \min\left\{D_{i,j}(k), P_{i,j}(k) S_{i+1}(k)\right\}, \tag{6}$$

where the demand $D_{i,j}$ of vehicle type j and supply S_i of all vehicle classes in cell i can be calculated as follows [14]:

$$D_{i,j}(k) = \begin{cases} u_i(k)\rho_{i,j}(k)\eta_{i,j}(k) & \text{if } \rho_{i,j}(k) \le \rho_{j,c} \\ Q_j & \text{if } \rho_{i,j}(k) > \rho_{j,c}, \end{cases} \tag{7}$$

$$S_i(k) = \begin{cases} Q_i & \text{if } E\rho_i(k) \le \rho_c \\ w\left(\rho_{jam}(k) - E\rho_i(k)\right) & \text{if } E\rho_i(k) > \rho_c, \end{cases} \tag{8}$$

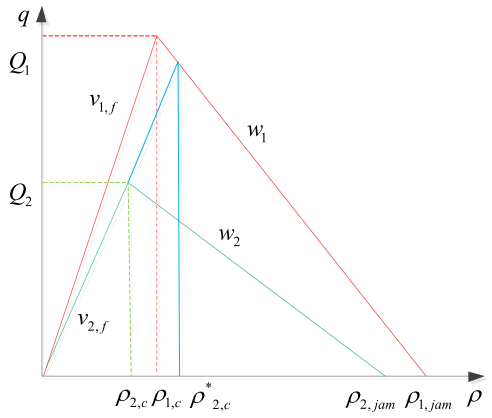

FIGURE 3. FD for two vehicle classes.

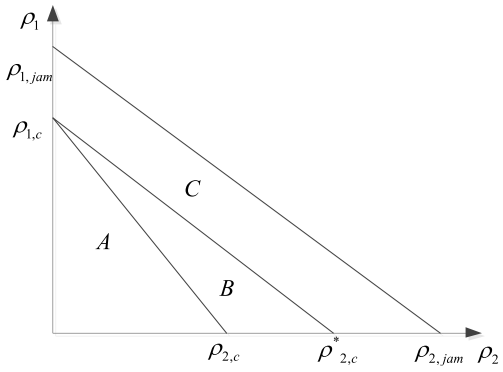

FIGURE 4. Three traffic conditions for two vehicle classes.

where $u_i(k)$ is the speed limit of cell i during time interval k, Q_j is the maximum demand of vehicle type j, w is the freeway backward shock wave speed, ρ_{jam} is the freeway jam density, and Q_i is the maximum supply of cell i.

To estimate $v_{i,j}(k)$, it is necessary to consider whether the traffic condition is free or congested. For clear clarification, we only include two types of vehicles here, i.e., cars and trucks. Vehicle Type 1 is "car" and Vehicle Type 2 refers to "truck". The free-flow speed of Vehicle Type 1 is greater than that of Vehicle Type 2, i.e., $v_{1,f} > v_{2,f}$. Fig. 3 shows the fundamental diagram (FD) for two vehicle types. The red line is for the FD of Vehicle Type 1, and the green line denotes the FD of Vehicle Type 2. $\rho_{j,jam}$, $\rho_{j,c}$, w_j, and $v_{j,f}$ are the jam density, critical density, wave speed, and maximum speed of vehicle type j, respectively. Density $\rho^*_{2,c}$ linking the FDs of the two vehicle types as shown in Fig. 3 by blue lines can be computed as [21], [28]:

$$\rho^*_{2,c} = \frac{w_1 \rho_{1,jam}}{w_1 - v_{2,f}}. \tag{9}$$

As the density of each type of vehicle ρ_j cannot exceed its jam density $\rho_{j,jam}$, three traffic conditions are differentiated according to the relationship between ρ_j and $\rho^*_{2,c}$, as shown in Fig. 4 [14], [21]. These three traffic conditions can help us to determine whether some types of vehicles are in congested traffic conditions or not. In this way, based on different traffic

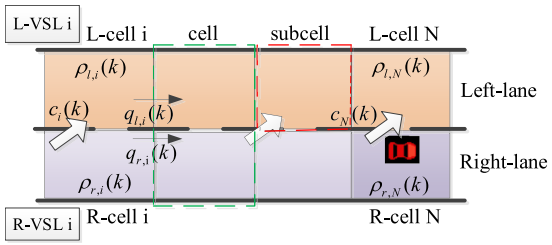

FIGURE 5. Cell stretch and configuration of integrated VSL and LC control system. The green dashed box indicates a cell and the red dashed box indicates a sub-cell.

conditions, we can have a more accurate speed prediction for different types of vehicles with the speed limit control $u_i(k)$ applied to the cell i during time interval k.

1) CONDITION A

If $(\rho_1/\rho_{1,c}) + (\rho_2/\rho_{2,c}) \leq 1$, both vehicle types are in a free flow state. The average speed of vehicle type j in cell i during time interval k is $v_{i,j}(k) = \min(v_{j,f}, u_i(k))$.

2) CONDITION B

From [28], in the multiple vehicle types setting, vehicle types with slower speed may be still in free flow states, while vehicle types with faster speed cannot drive by free flow speed, that is, faster vehicle types are in a congestion state. This traffic condition is called semi-condition [14], [28]. Under this condition, the actual speed of slower vehicle types in free flow is less than or equal to the actual speed of faster vehicle types in congested mode. According to [21], $\rho^*_{2,c}$ is the boundary condition distinguishing the semi-congestion condition from the congestion condition. From [21], if $(\rho_1/\rho_{1,c}) + (\rho_2/\rho_{2,c}) > 1$ and $(\rho_1/\rho^*_{2,c}) + (\rho_2/\rho_{2,c}) \leq 1$, Vehicle Type 1 is in a congested traffic condition and Vehicle Type 2 is in a free flow condition. According to [14], the average speed of Vehicle Type 1 in cell i is $v_{i,1}(k) = \{w(\rho_{jam} - E\rho_i(k))\}/E\rho_i(k)$, and the average speed of Vehicle Type 2 in cell i is $v_{i,2}(k) = \min(v_{2,f}, u_i(k))$.

3) CONDITION C

If $(\rho_1/\rho^*_{2,c}) + (\rho_2/\rho_{2,c}) > 1$ and $(\rho_1/\rho_{1,jam}) + (\rho_2/\rho_{2,jam}) \leq 1$, both vehicle types are in a congested traffic condition, where $\rho_{j,jam} = \rho_{1,jam}/\eta_{j,jam}$ and $\eta_{j,jam} = sd_j/sd_{car}$. Their speeds are the same and less than the actual speed of slower vehicle types. Their speeds are as follows: $v_{i,j}(k) = \{w(\rho_{jam} - E\rho_i(k))\}/E\rho_i(k)$.

The space mean speed $v_{i,j}(k)$ of vehicle type j in cell i can be calculated according to above three conditions.

Above all is the whole multi-class CTM framework for predicting density, flow, and speed in each cell. For more details about the original multi-class CTM, interested readers are referred to [14].

B. IMPROVED MULTI-CLASS CTM

We improve the original multi-class CTM based on DPCEs to meet our lane-level control and incorporate LC control, since the original multi-class CTM does not consider the effect of LC control.

The divisions of cells in existing work are mostly at the road level, i.e., different lanes of the same road segment are in a cell. To achieve our lane-level control objective, we divide road cells into sub-cells further at the lane-level, i.e., different lanes of the same road segment are different sub-cells, as shown in Fig. 5. The green dashed box indicates a cell, and the red dashed box indicates a sub-cell. In this way, we can provide more specific service on lane-level by sending different speed change information to different lanes on road segments. As shown in Fig. 5, light orange sub-cells are sub-cells on the left lane and light purple sub-cells are sub-cells on the right lane. The dark purple sub-cell means that the incident happens in this sub-cell. $v_{l,i,j}$ and $\rho_{l,i,j}$ are the average speed and density of vehicle type j in the ith left sub-cell. $q^{i,i+1}_{l,j}(k)$ is the flow of vehicle type j from left sub-cell i to left sub-cell $i+1$. $v_{r,i,j}$ and $\rho_{r,i,j}$ are average speed and density of vehicle type j in the ith right sub-cell. $q^{i,i+1}_{r,j}(k)$ is the flow of vehicle type j from right sub-cell i to right sub-cell $i+1$.

The demand function in sub-cell i can still be calculated as (7). There is a difference in calculating the supply of sub-cell i. We assume Q_s is the maximum capacity of sub-cells. The maximum capacity in the Nth right sub-cell where the incident car is located is zero, i.e., $Q_s = 0$, and the maximum capacity in other sub-cells is $1/2Q$, i.e., $Q_s = 1/2Q$. So the supply function is turned into:

$$S_i(k) = \begin{cases} Q_s & \text{if } E\rho_i(k) \leq \rho_c \\ w(\rho_{jam}(k) - E\rho_i(k)) & \text{if } E\rho_i(k) > \rho_c. \end{cases} \quad (10)$$

From above, we can calculate the demand function and supply function in each sub-cell.

We make extensions to (4) by considering the impact of LC vehicles. Because of LC control, there are $c_{i,j}(k)$ vehicles traveling from right-lane sub-cell i to left-lane sub-cell i within a time of T, so the density function in left-lane sub-cell i of vehicle type j during time interval k is:

$$\rho_{l,i,j}(k+1) = \rho_{l,i,j}(k) + \frac{1}{l}c_{i,j}(k) + \frac{T}{l}\left(q^{i-1,i}_{l,j}(k) - q^{i,i+1}_{l,j}(k)\right), \quad (11)$$

and the density function in right-lane sub-cell i of vehicle type j during time interval k is:

$$\rho_{r,i,j}(k+1) = \rho_{r,i,j}(k) - \frac{1}{l}c_{i,j}(k) + \frac{T}{l}\left(q^{i-1,i}_{r,j}(k) - q^{i,i+1}_{r,j}(k)\right), \quad (12)$$

where $q^{i,i+1}_{l,j}(k)$ and $q^{i,i+1}_{r,j}(k)$ can be calculated according to (6). So based on the original multi-class CTM and our extensions, the density, flow, and speed in each sub-cell can be predicted.

IV. THE GA BASED TRAFFIC CONTAOL

We choose MPC for online traffic control, due to the robustness of MPC. In our combined VSL and LC control method, the values of speed limits in sub-cells and numbers of LC vehicles in cells are our decision variables. An objective function considering overall traffic efficiency is used to capture the future performance of the system to be controlled over some prediction horizon. Then a GA based strategy is adopted to optimize the value of the objective function. According to the receding horizon scheme of MPC, only the element in the first control horizon of this optimal input sequence is applied to the controlled system. After that, vehicles will change states according to the received speed information, LC information, and surrounding road conditions as well.

We notice that when the incident is over, upstream vehicles that follow VSL information cannot speed up to the maximum speed immediately, resulting in a decrease in the utilization of road capacity. So when the incident is almost over, the incident vehicle sends the maximum speed limit v_f to CAVs upstream. Though it is a simple idea, this innovation can effectively improve road traffic efficiency immediately after the incident is over.

A. OPTIMIZATION PROBLEM

The purpose of our control method is to find the control signals $u_{l,i}(k)$, $u_{r,i}(k)$, and $c_i(k)$ that minimize an objective function about the future performance. $u_{l,i}(k)$, $u_{r,i}(k)$, and $c_i(k)$ are the controlled left sub-cell speed limit value, right sub-cell speed limit value, and the number of LC vehicles in the ith cell. According to MPC, our control computes optimal speed limits and numbers of LC vehicles during a prediction horizon N_p, and implements them in SUMO for a control horizon N_c. $N_p = T_p/T$, $N_c = T_c/T$, and $N_c \leq N_p$, where T_p and T_c are times for prediction and control, respectively. The first prediction horizon is $k = 1, 2, \ldots, N_p$ and the first control horizon is $k = 1, 2, \ldots, N_c$. After that, the second prediction horizon is $k = N_c + 1, N_c + 2, \ldots, N_c + N_p$, and the second control horizon is $k = N_c + 1, N_c + 2, \ldots, 2N_c$. So the nth prediction horizon is from $(n-1)N_c + 1$ to $(n-1)N_c + N_p$, and the nth control horizon is from $(n-1)N_c + 1$ to nN_c. We use the improved multi-class CTM to predict the density, speed, and flow rate of each sub-cell from $(n-1)N_c + 1$ to $(n-1)N_c + N_p$ under these control signals. The objective function of our integrated control method is set as the weighted sum of TTS and TTD, to comprehensively improve traffic mobility and efficiency. TTS can reflect the waiting time and driving time of all vehicles, while TTD can reflect the travel distance of all vehicles.

Considering LC maneuvers can disrupt the traffic flow, we make these LC maneuvers as evenly distributed among cells as possible, rather than concentrating maneuvers in one cell. Here is a simple example to illustrate our idea. Suppose there are two kinds of LC control: A) There are no vehicles changing lanes in the first cell and 20 vehicles changing lanes in the second cell; B) There are 10 vehicles changing lanes in the first cell and the second cell respectively. From a traffic engineering point of view, B) control is better than A) control. On the one hand, because vehicles need to find appropriate gaps to change lanes, there are longer waiting time of LC vehicles in A) control than in B) control. On the other hand, many LC maneuvers in the second cell increase the interaction between vehicles on different lanes, leading to frequent acceleration and deceleration behaviors of vehicles, which seriously reduces traffic efficiency. We therefore try to distribute LC maneuvers among different cells and make c_i not change too often from one cell to the other.

In addition, considering passenger comfort and to prevent excessive speed changes between adjacent sub-cells, we add terms about speed change between different adjacent cells to the objective function to smooth speed transmission from upstream to downstream.

To maintain the ideal capacity of the bottleneck after an incident, we try to make the speed limit in the Nth left sub-cell be constant and equal to v_f, i.e., $u_{l,N}(k) = v_f$. In addition, to reduce the waiting time in the Nth right sub-cell, we make the number of LC vehicles in cell N be the number of vehicles in the Nth right sub-cell. The other speed limits and numbers of LC vehicles in other controlled sub-cells are decision variables that need to be solved.

When the speed limit is too small, it may induce wide moving jam (WMJ) and exaggerate congestions [29]. Considering the operating efficiency and the maximum speed limit of a freeway, all $u_{l,i}(k)$ and $u_{r,i}(k)$ should be greater than a predefined minimum value v_{min} and less than the maximum freeway speed limit v_f. Considering the comfort of passengers and acceleration limitation, the speed change between two consecutive time steps should not be larger than a predefined value a_d. The optimization problem is:

$$\begin{aligned}
\min\ J = {} & \alpha_1 Tl \sum_{k=(n-1)N_c+1}^{(n-1)N_c+N_p} \sum_{i=1}^{N} \sum_{j=1}^{J} \left(\rho_{r,i,j}(k) + \rho_{l,i,j}(k)\right) \\
& - \alpha_2 Tl \sum_{k=(n-1)N_c+1}^{(n-1)N_c+N_p} \sum_{i=1}^{N} \sum_{j=1}^{J} \left(\rho_{r,i,j}(k) v_{r,i,j}(k)\right) \\
& - \alpha_2 Tl \sum_{k=(n-1)N_c+1}^{(n-1)N_c+N_p} \sum_{i=1}^{N} \sum_{j=1}^{J} \left(\rho_{l,i,j}(k) v_{l,i,j}(k)\right) \\
& + \sum_{k=(n-1)N_c+1}^{(n-1)N_c+N_p} \sum_{i=1}^{N-1} \left(c_{i+1}(k) - c_i(k)\right)^2 \\
& + \sum_{k=(n-1)N_c+1}^{(n-1)N_c+N_p} \sum_{i=1}^{N-1} \left(u_{l,i+1}(k) - u_{l,i}(k)\right)^2 \\
& + \sum_{k=(n-1)N_c+1}^{(n-1)N_c+N_p} \sum_{i=1}^{N-1} \left(u_{r,i+1}(k) - u_{r,i}(k)\right)^2, \qquad (13a)
\end{aligned}$$

$$\text{s.t. } u_{l,N}(k) = v_f, \qquad (13b)$$

$$c_N(k) = T q_{r,N-1}(k), \qquad (13c)$$

$$v_{min} \leq u_{l,i}(k) \leq v_f, \qquad (13d)$$

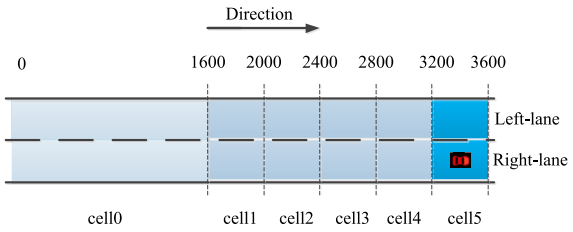

FIGURE 6. Schematic diagram of the simulation scenario.

$$v_{min} \le u_{r,i}(k) \le v_f, \tag{13e}$$
$$0 \le c_i(k) \le Tq_{r,i-1}(k), \tag{13f}$$
$$\left|u_{r,i}(k) - u_{r,i}(k-1)\right| \le a_d, \tag{13g}$$
$$\left|u_{l,i}(k) - u_{l,i}(k-1)\right| \le a_d, \tag{13h}$$

where α_1 and α_2 are weighting parameters for TTS and TTD, respectively. $\rho_{r,i,j}(k+1)$ and $\rho_{l,i,j}(k+1)$ in (13a) are calculated by the density $\rho_{r,i,j}(k)$ and $\rho_{l,i,j}(k)$ according to two density renewal formulas (11) and (12) in our improved multi-class CTM. According to the three traffic conditions in Section III-A, $v_{r,i,j}(k)$ and $v_{l,i,j}(k)$ in (13a) are easy to be calculated based on $\rho_{r,i,j}(k)$ and $\rho_{l,i,j}(k)$.

B. GA-BASED SOLUTION ALGORITHM

The above optimization problem is a general nonconvex problem. To efficiently solve the above MPC problem, one of the most commonly used metaheuristic search algorithms, GA, is selected to optimize the problem for its simplicity and efficiency. Interested readers are referred to [30] for a full description of the GA. Using the information of CAVs, average speed, density, and flow rate in each cell are collected. The GA repeatedly generates a population of individual solutions. These individual solutions are evaluated based on the objective function value (13a) in the next prediction horizon according to the modified multi-class CTM with these collected data. The decision variables on the controlled segments during time interval k can be represented by

$$\mathbf{U}(k) = (u_{r,1}(k), \ldots, u_{r,i}(k), \ldots, u_{r,N}(k), u_{l,1}(k), \ldots, u_{l,i}(k), \ldots, u_{l,N}(k), c_1(k), \ldots, c_i(k), \ldots, c_N(k)).$$

To reduce the amount of calculation, we make $u_{l,i}(k), u_{r,i}(k) \in \{3, 6, 9, \ldots, 30, 33\}$. In each predicted horizon, the GA outputs the optimal solution $\mathbf{U}_{optimal}(k)$ after many generations, where $k = (n-1)N_c + 1, \ldots, (n-1)N_c + N_p$. The $\mathbf{U}_{optimal}(k)$ is sent to SUMO through TraCI, and CAVs change their states according to the $\mathbf{U}_{optimal}(k)$ in a control horizon N_c.

V. SIMULATIONS AND RESULTS

A. SIMULATION NETWORK AND SCENARIOS

We evaluate the combined control method of a two-lane freeway in SUMO which has a static speed limit of 120 km/h (33.3 m/s). Other road parameters are SUMO default values. Its maximum traffic capacity without an incident is about 4600 PCE/h/2lanes and the critical density is 46 PCE/km/2lanes. We assume the bottleneck is introduced by an incident that blocks the right lane in the two-lane freeway, thus the ideal capacity of the bottleneck during the incident is about 2300 PCE/h/2lanes. However, the actual capacity is only about 1270 PCE/h/2lanes due to the effects of the capacity drop phenomenon. Assuming that the incident car stops at 3400 m and the upstream segment of the bottleneck is divided into 5 parts of 400 m sections, from cell 1 to cell 5, just as Fig. 6 shows. The simulation step in SUMO is 1 s and the discrete time step T in our control method is 10 s. The prediction horizon T_p is 5 min and the control horizon T_c is 1 min. A 100 min simulation with a 10 min warm-up time and a 1.6 km warm road length is conducted. Other basic parameters of the two-lane freeway are shown in Table 1. In our method, we focus on reducing the TTS, which means reducing the waiting time and the running time of vehicles. Accordingly, we set $\alpha_1 = 0.8$ and $\alpha_2 = 0.2$. We set the predefined minimum speed limit $v_{min} = 3$ m/s and the predefined speed change limit between two consecutive controlled moments $a_d = 3$.

TABLE 1. The basic parameters of the two-lane freeway.

Parameter	Value
Capacity (PCE/h/2lanes)	4600
Drop Capacity (PCE/h/2lanes)	1270
Critical density (PCE/km/2lanes)	46
Jam density (PCE/km/2lanes)	260
Car	
Free-flow speed (km/h)	120
Critical density (PCE/km/2lanes)	46.9
Jam density (PCE/km/2lanes)	260
Truck	
Free-flow speed (km/h)	85
Critical density (PCE/km/2lanes)	40.7
Jam density (PCE/km/2lanes)	133

The car-following model and LC model we use in SUMO are "Krauss" [31] and "LC2013" [32], respectively. The LC in SUMO is instantaneous and completed in a single simulation step. However, an LC maneuver generally takes longer than a single simulation step. So we set the option "lanechange.duration" in SUMO and activate a simple continuous LC model. Although this will make the simulation run longer, it can better describe the impact of LC behaviors on traffic efficiency. To simulate differences in driver behaviors, vehicle speeds obey a truncated normal distribution, where the expectation is the free-flow speed of the vehicle and the variance is 0.1 m^2/s^2. The upper and lower bounds are set according to the actual situation. The response time of drivers also accords with a truncated normal distribution. Due to the differences in driver behaviors and other factors, traffic flow has a stochastic feature [29]. Therefore, we perform 10 experiments for each group and obtain the average results of them.

B. SIMULATION RESULTS UNDER DIFFERENT TRAFFIC DEMANDS

To compare the effects with and without our control, simulations under low, middle and high traffic demands (1000,

TABLE 2. Evaluation results under different demands.

Traffic demand (PCE/h/2lanes)	Flow (PCE/h/2lanes)		
	No control	No control	Change rate
1000	1036	1010	−2.5%
2000	1090	1647	51.1%
3000	892	2226	149.5%

2000, and 3000 PCE/h/2lanes respectively) are run. The low traffic demand 1000 PCE/h/2lanes is lower than the reduced capacity 1270 PCE/h/2lanes. The middle traffic demand 2000 PCE/h/2lanes is between 1270 PCE/h/2lanes and the ideal one lane capacity 2300 PCE/h/2lanes. The high traffic demand 3000 PCE/h/2lanes is higher than 2300 PCE/h/2lanes. These three simulations are run under a scenario where there is a lane closure caused by road construction. The metric of flow is adopted to analyze the results.

The results without and with control are shown in Table 2. For low traffic demand (1000 PCE/h/2lanes), the flow has a little change from 1036 to 1010 PCE/h/2lanes (−2.5%). However, for middle demand (2000 PCE/h/2lanes), the flow improves a lot, changing from 1090 to 1647 PCE/h/2lanes (51.1%). The significant improvement is especially noticeable in high demand (3000 PCE/h/2lanes), where the flow is increased from 892 to 2226 PCE/h/2lanes (149.5%). When the traffic demand is lower than the reduced capacity, vehicles can run smoothly on the road. There is no need to control traffic if the traffic demand is lower than the reduced capacity. When the traffic demand is higher than the reduced capacity, the increased interaction between vehicles makes it easy for the traffic at the bottleneck to collapse, resulting in a flow of less than 1270 PCE/h/2lanes. Under these traffic demands, our control can reduce the capacity drop phenomenon by distributing LC maneuvers and significantly improve traffic efficiency.

To further study the performance of our integrated control, we investigate the capacity of the road, i.e., when the maximum flow rate. For clarity of comparison, the relationship between the flow and the density upstream of the bottleneck is presented in Fig. 7. The blue dotted line describes the FD under our integrated control. The red line shows the corresponding FD without control. As Fig. 7 illustrates, our control improves the maximum volume of traffic from 12.8 PCE/km to 22.3 PCE/km and the maximum flow rate from 1270 PCE/h to 2228 PCE/h. The results in Table 3 and Fig. 7 point up that our method indeed helps to improve road capacity.

C. SIMULATION RESULTS UNDER DIFFERENT INCIDENT SCENARIOS

To demonstrate the robustness and applicability of our proposed control method, we design three scenarios to test our method. In each scenario, the incident occurs 10 minutes after the simulation experiment begins. In scenario 1, the incident lasts for 10 min to simulate a vehicle breakdown or a minor incident. In scenario 2, the incident lasts for 30 min which simulates a normal incident. In scenario 3, the incident is

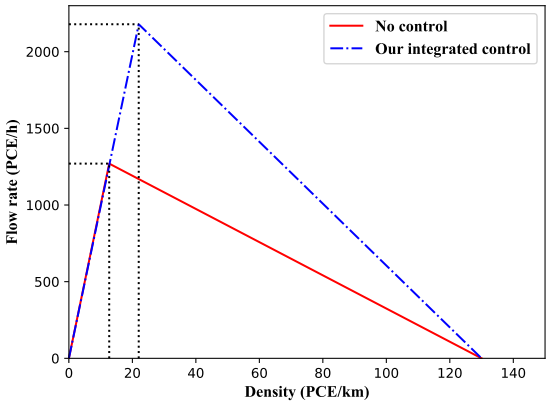

FIGURE 7. FD diagram with and without our integrated control.

not removed to simulate a construction site or a physical bottleneck. These three scenarios are run under a constant traffic demand of 3000 PCE/h/2lanes which is higher than the capacity of the bottleneck.

We compare our method with no control and VSL-only control. VSL-only control does not consider LC vehicles and distinguish lanes for control. It sends speed limits to cells upstream of the bottleneck based on the original multi-class CTM. To analyze the simulation results and compare the performances of the network under uncontrolled and controlled scenarios, TTS, TTD, and average exhaust emissions are used as shown in Tables 3, 4, and 5. Considering the shock wave dissipation, the statistical period is the time from the occurrence of the incident to the time of 10 minutes after the incident is relieved. Average emissions rates are calculated based on the HBEFA3 model [33]. Tables 3, 4, and 5 show that the improvements in TTS and average emissions are significant under our integrated control. In scenarios 1, 2, and 3, the improvement percentages of TTS are 23.56%, 44.62%, and 27.25%, respectively. These improvements outperform improvement with VSL-only control, which are 9.16%, 13.84%, and 6.43%, respectively. The reason for this is that our integrated control method distributes LC maneuvers and reduces interaction between vehicles. This reduces the degree of traffic congestion and waiting time, which leads to a significant improvement in TTS. In three scenarios, the emissions of CO_2, PMx, NOx, and fuel decrease by 11.23% − 44.68%, 10.29% − 48.19%, 12.32%−26.65%, and 11.23%−44.68%, respectively. Under VSL-only control, the emissions of CO_2, PMx, NOx, and fuel decrease by 4.45% − 26.24%, 4.84% − 30.67%, 4.85% − 27.62%, and 4.45% − 26.24%, respectively. The decrease in emissions with our integrated control is far superior to VSL-only control. The results point up that our integrated control can bring many environmental benefits. Here are two perspectives to illustrate this. First, it reduces the waiting time of vehicles, and therefore decreases the exhaust emissions of vehicles waiting in the queue. Second, it harmonizes vehicle speed and reduces the acceleration and deceleration behaviors of vehicles, which decreases exhaust emissions caused by these acceleration and deceleration behaviors.

TABLE 3. Evaluation results of scenario 1.

Control	No control	VSL-only control		Our integrated control	
	Value	Value	Change rate	Value	Change rate
TTS (s)	967684.00	878976.00	−9.16%	736784.00	−23.86%
TTD (m)	21236400.00	21236400.00	0.00%	21265200.00	13.56%
Average CO_2 (mg)	649132.00	620234.14	−4.45%	576225.43	−11.23%
Average PMx (mg)	14.49	13.78	−4.84%	12.99	−10.29%
Average NOx (mg)	263.12	250.36	−4.85%	230.69	−12.32%
Average fuel (mg)	279.03	266.61	−4.45%	247.69	−11.23%

TABLE 4. Evaluation results of scenario 2.

Control	No control	VSL-only control		Our integrated control	
	Value	Value	Change rate	Value	Change rate
TTS (s)	1790989.00	1543174.00	−13.84%	991890.00	−44.62%
TTD (m)	21286800.00	21229200.00	−0.27%	21243600.00	−0.20%
Average CO_2 (mg)	896285.24	817525.33	−8.78%	671941.66	−25.03%
Average PMx (mg)	19.64	17.65	−10.13%	14.94	−23.91%
Average NOx (mg)	372.33	336.85	−9.75%	273.01	−26.65%
Average fuel (mg)	385.28	351.43	−8.79%	288.84	−25.03%

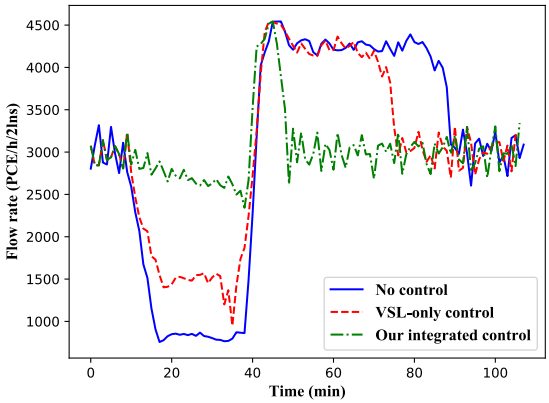

FIGURE 8. Average flow under different control methods.

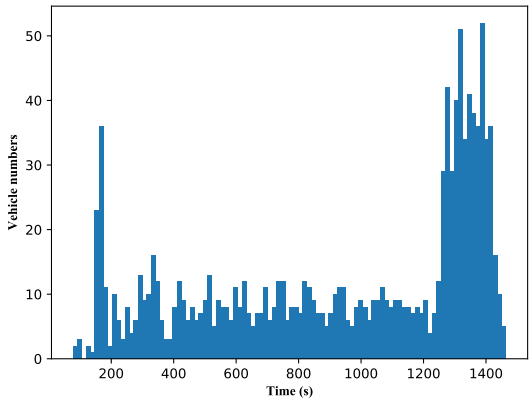

FIGURE 9. Distribution of duration in scenario 2 without control.

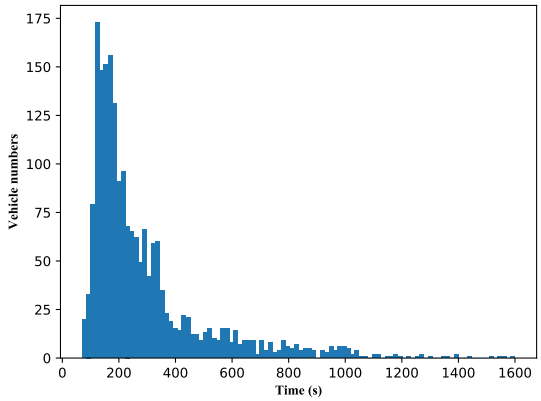

FIGURE 10. Distribution of duration in scenario 2 with the integrated control.

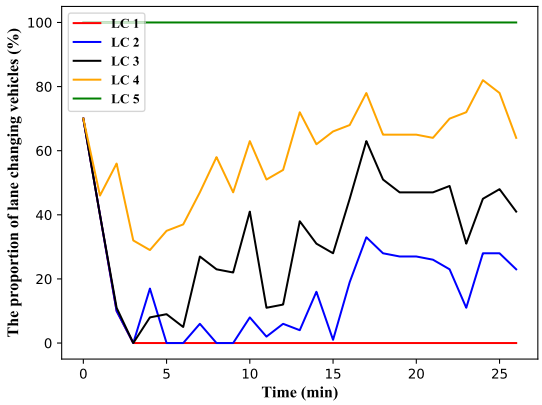

FIGURE 11. The proportion of LC vehicles of the integrated control method in scenario 2.

From Tables 3, 4, and 5, it can be seen that the longer the incident lasts, the greater the reduction in emissions is.

Our control goal is to increase TTD. However, in scenario 2, TTD does not increase but decreases by −0.20%. This result is related to the weighting factors we set. We lay more emphasis on reducing TTS than increasing TTD. Although TTD decreases in scenario 2, the decrease of TTD is small and acceptable compared to the improvement of reduction in TTS.

To further compare our integrated control method with other methods, we plot the average flow of scenario 2 under different control methods as shown in Fig. 8. The average flow is obtained by averaging the flow rate of five controlled road segments. Fig. 8 shows that, from 10 min to 40 min, i.e., the incident car blocks one lane, the flow rate of the bottleneck is far less than 1000 PCE/h/2lanes. The VSL-only method improves the flow rate to about 1500 PCE/h/2lanes.

TABLE 5. Evaluation results of scenario 3.

Control	No control	VSL-only control		Our integrated control	
	Value	Value	Change rate	Value	Change rate
TTS (s)	3012887.00	2819107.99	−6.43%	2191805.99	−27.25%
TTD (m)	8276400.00	11977200.00	44.71%	18583200.00	124.53%
Average CO_2 (mg)	2123528.92	1566282.71	−26.24%	1174667.79	−44.68%
Average PMx (mg)	47.45	32.90	−30.67%	24.58	−48.19%
Average NOx (mg)	929.53	672.78	−27.62%	493.76	−46.88%
Average fuel (mg)	912.85	673.29	−26.24%	504.94	−44.684%

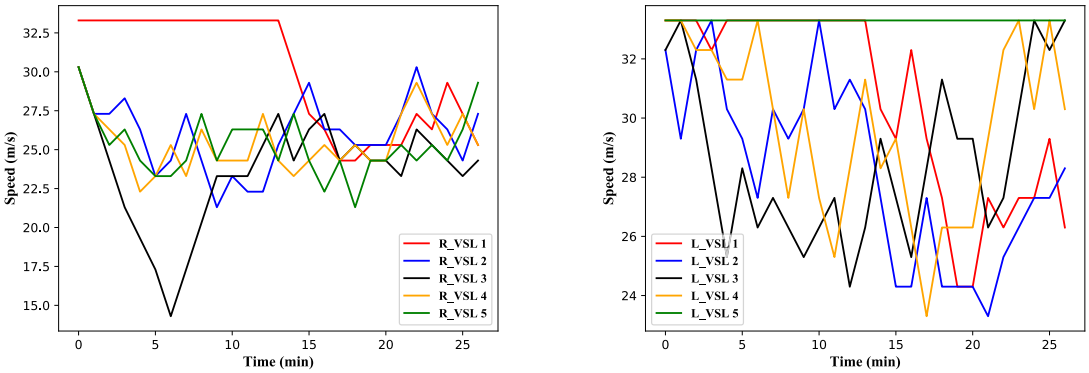

FIGURE 12. The speed limits of the integrated control method in scenario 2. (a) The speed limits in right sub-cells; (b) The speed limits in left sub-cells.

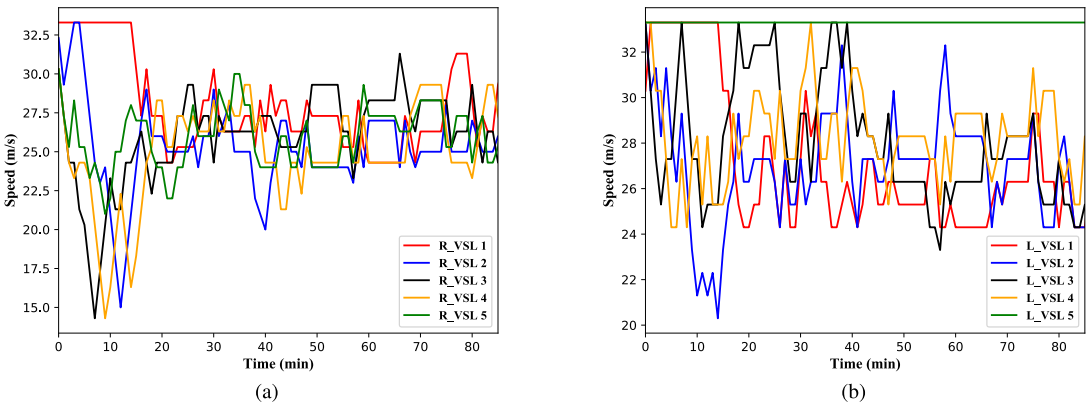

FIGURE 13. The speed limits of the integrated control method in scenario 3. (a) The speed limits in right sub-cells; (b) The speed limits in left sub-cells.

Our integrated control method can improve the flow rate to nearly 2750 PCE/h/2lanes, which outperforms the VSL-only method. It can be seen that our integrated control can improve the discharge flow compared with no control and VSL-only control. There are some jitters in the flow at about 35 min to 40 min due to the adopted maximum speed control on all controlled sections when the incident is almost over. When the incident is cleared, i.e., from 40 min, the average flow would return to normal level soon under the integrated control method as there are fewer vehicles queuing in the road compared with no control and VSL-only control. It means the integrated control method can reduce the queue size significantly. We test other scenarios under different traffic demands, and the conclusions remain unchanged.

To compare the effects of the integrated control on individual cars, we plot the distribution of duration. The duration is the total time that takes a vehicle to pass all sections of the road. It includes the waiting time, which is the time during which the vehicle speed is below 0.1 m/s. So the duration indicator can reflect not only the speed of the vehicle but also the waiting time.

Fig. 9 is the distribution of duration without control in scenario 2, while Fig. 10 is the distribution of duration with our integrated control in scenario 2. In Fig. 9, the duration of many vehicles is concentrated between 1200 s and 1400 s, which means there are many vehicles queuing for a long time. Whereas in Fig. 10, there are fewer vehicles concentrated between 1200 s and 1400 s and many vehicles have a duration of about 200 s. From these two figures, we can draw that the integrated control significantly reduces the waiting time of many vehicles and improves traffic efficiency.

The proportion of LC vehicles is the ratio of the calculated number of LC vehicles and the total number of vehicles in each cell. When analyzing the proportion of LC vehicles, we find that the proportion in the first control segment and the second control segment are close to 0 in scenario 1 as time goes on. The proportion in the first control segment converges to 0 in scenario 2, which is shown in Fig. 11. This means there is no need to control vehicles to change lanes in segments where the proportion is zero. It can be inferred that the duration of the incident affects the length of the LC control road segments.

If we divide the cells with shorter lengths, we can figure out the length of LC controlled segments. In this way, the length of LC controlled segments is solved by GA. Compared with methods in [10], which is solved through simulation, our method of figuring out the length of LC controlled segments may be more efficient. Furthermore, analyzing the speed limits calculated from our integrated control, we find that speed limits from right sub-cell 1 to right sub-cell 5 converge to 22-27 m/s, which is shown in Fig. 12 (a). The phenomenon is even more obvious when the control time gets longer, as shown in Fig. 13 (a). However, there is no convergence of speed limits in left sub-cells, as shown in Fig. 12 (b) and Fig. 13 (b). In the future, we will conduct further studies on this phenomenon.

VI. CONCLUSION

We propose a new refined integrated VSL and LC control method aiming at freeway bottlenecks under mixed traffic flows in this paper. Our work is in the framework of MPC and can consider the interaction between VSL and LC to maximize traffic efficiency. We improve a multi-class CTM by considering the impact of LC behaviors to predict traffic state better. Then we employ a GA-based method to find the optimal values of VSL and LC numbers simultaneously during each horizon. Simulation results demonstrate that our control method can improve the capacity of the road and provide significant improvements in traffic mobility and exhaust emissions. Our control method can reduce TTS greatly by 23.86% to 44.62% which outperforms the VSL-only control.

In future work, we plan to study traffic scenarios with different penetration rates of CAVs. We will consider the difference between traditional human-driven vehicles and CAVs and propose a robust control method for different penetration rates of CAVs.

REFERENCES

[1] J. H. Banks, "The two-capacity phenomenon: Some theoretical issues," *Transp. Res. Rec.*, no. 1320, pp. 234–241, 1991.
[2] C. Zhang, N. R. Sabar, E. Chung, A. Bhaskar, and X. Guo, "Optimisation of lane-changing advisory at the motorway lane drop bottleneck," *Transp. Res. C, Emerg. Technol.*, vol. 106, pp. 303–316, Sep. 2019.
[3] L. Leclercq, V. L. Knoop, F. Marczak, and S. P. Hoogendoorn, "Capacity drops at merges: New analytical investigations," *Transp. Res. C, Emerg. Technol.*, vol. 62, pp. 171–181, Jan. 2016.
[4] M. J. Cassidy and J. Rudjanakanoknad, "Increasing the capacity of an isolated merge by metering its on-ramp," *Transp. Res. B, Methodol.*, vol. 39, no. 10, pp. 896–913, Dec. 2005.
[5] A. Hegyi, B. De Schutter, and H. Hellendoorn, "Model predictive control for optimal coordination of ramp metering and variable speed limits," *Transp. Res. C, Emerg. Technol.*, vol. 13, no. 3, pp. 185–209, Jun. 2005.
[6] P. Allaby, B. Hellinga, and M. Bullock, "Variable speed limits: Safety and operational impacts of a candidate control strategy for freeway applications," *IEEE Trans. Intell. Transp. Syst.*, vol. 8, no. 4, pp. 671–680, Dec. 2007.
[7] J. R. D. Frejo, I. Papamichail, M. Papageorgiou, and B. De Schutter, "Macroscopic modeling of variable speed limits on freeways," *Transp. Res. C, Emerg. Technol.*, vol. 100, pp. 15–33, Mar. 2019.
[8] J. A. Laval and C. F. Daganzo, "Lane-changing in traffic streams," *Transp. Res. B, Methodol.*, vol. 40, no. 3, pp. 251–264, Mar. 2006.
[9] C. Roncoli, I. Papamichail, and M. Papageorgiou, "Hierarchical model predictive control for multi-lane motorways in presence of vehicle automation and communication systems," *Transp. Res. C, Emerg. Technol.*, vol. 62, pp. 117–132, Jan. 2016.
[10] Y. Zhang and P. A. Ioannou, "Combined variable speed limit and lane change control for truck-dominant highway segment," in *Proc. IEEE 18th Int. Conf. Intell. Transp. Syst.*, Sep. 2015, pp. 1163–1168.
[11] Y. Zhang and P. A. Ioannou, "Combined variable speed limit and lane change control for highway traffic," *IEEE Trans. Intell. Transp. Syst.*, vol. 18, no. 7, pp. 1812–1823, Jul. 2017.
[12] B. Khondaker and L. Kattan, "Variable speed limit: A microscopic analysis in a connected vehicle environment," *Transp. Res. C, Emerg. Technol.*, vol. 58, pp. 146–159, Sep. 2015.
[13] J. Nie, J. Zhang, W. Ding, X. Wan, X. Chen, and B. Ran, "Decentralized cooperative lane-changing decision-making for connected autonomous vehicles*," *IEEE Access*, vol. 4, pp. 9413–9420, 2016.
[14] M. Yu and W. D. Fan, "Optimal variable speed limit control in connected autonomous vehicle environment for relieving freeway congestion," *J. Transp. Eng. A, Syst.*, vol. 145, no. 4, Apr. 2019, Art. no. 04019007.
[15] M. Wang, W. Daamen, S. P. Hoogendoorn, and B. van Arem, "Connected variable speed limits control and car-following control with vehicle-infrastructure communication to resolve stop-and-go waves," *J. Intell. Transp. Syst.*, vol. 20, no. 6, pp. 559–572, Nov. 2016.
[16] E. N. Holland and A. W. Woods, "A continuum model for the dispersion of traffic on two-lane roads," *Transp. Res. B, Methodol.*, vol. 31, no. 6, pp. 473–485, Nov. 1997.
[17] A. Messmer and M. Papageorgiou, "METANET: A macroscopic simulation program for motorway networks," *Traffic Eng. Control*, vol. 31, no. 9, pp. 466–470, 1990.
[18] J. Van Lint, S. P. Hoogendoorn, and M. Schreuder, "FASTLANE: New multiclass first-order traffic flow model," *Transp. Res. Rec.*, vol. 2088, no. 1, pp. 177–187, 2008.
[19] P. Deo, B. De Schutter, and A. Hegyi, "Model predictive control for multi-class traffic flows," *IFAC Proc. Volumes*, vol. 42, no. 15, pp. 25–30, 2009.
[20] C. Pasquale, I. Papamichail, C. Roncoli, S. Sacone, S. Siri, and M. Papageorgiou, "Two-class freeway traffic regulation to reduce congestion and emissions via nonlinear optimal control," *Transp. Res. C, Emerg. Technol.*, vol. 55, pp. 85–99, Jun. 2015.
[21] S. Liu, H. Hellendoorn, and B. De Schutter, "Model predictive control for freeway networks based on multi-class traffic flow and emission models," *IEEE Trans. Intell. Transp. Syst.*, vol. 18, no. 2, pp. 306–320, Feb. 2017.
[22] S. Gashaw, P. Goatin, and J. Härri, "Modeling and analysis of mixed flow of cars and powered two wheelers," *Transp. Res. C, Emerg. Technol.*, vol. 89, pp. 148–167, Apr. 2018.
[23] M. Hadiuzzaman and T. Z. Qiu, "Cell transmission model based variable speed limit control for freeways," *Can. J. Civil Eng.*, vol. 40, no. 1, pp. 46–56, Jan. 2013.
[24] M. Carey, C. Balijepalli, and D. Watling, "Extending the cell transmission model to multiple lanes and lane-changing," *Netw. Spatial Econ.*, vol. 15, no. 3, pp. 507–535, Sep. 2015.
[25] H. H. S. N. Subraveti, V. L. Knoop, and B. van Arem, "First order multi-lane traffic flow model—An incentive based macroscopic model to represent lane change dynamics," *Transportmetrica B, Transp. Dyn.*, vol. 7, no. 1, pp. 1758–1779, 2019.
[26] T. Pan, W. H. K. Lam, A. Sumalee, and R. Zhong, "Multiclass multilane model for freeway traffic mixed with connected automated vehicles and regular human-piloted vehicles," *Transportmetrica A, Transp. Sci.*, to be published, doi: 10.1080/23249935.2019.1573858.
[27] K. Tiaprasert, Y. Zhang, C. Aswakul, J. Jiao, and X. Ye, "Closed-form multiclass cell transmission model enhanced with overtaking, lane-changing, and first-in first-out properties," *Transp. Res. C, Emerg. Technol.*, vol. 85, pp. 86–110, Dec. 2017.

[28] S. Liu, B. De Schutter, and H. Hellendoorn, "Model predictive traffic control based on a new multi-class METANET model," *IFAC Proc. Volumes*, vol. 47, no. 3, pp. 8781–8786, 2014.
[29] Y. Wang, Y. Zhang, J. Hu, and L. Li, "Using variable speed limits to eliminate wide moving jams: A study based on three-phase traffic theory," *Int. J. Modern Phys. C*, vol. 23, no. 9, 2012, Art. no. 1250060.
[30] K. Deb, A. Pratap, S. Agarwal, and T. Meyarivan, "A fast and elitist multiobjective genetic algorithm: NSGA-II," *IEEE Trans. Evol. Comput.*, vol. 6, no. 2, pp. 182–197, Apr. 2002.
[31] S. Krauß, "Microscopic modeling of traffic flow: Investigation of collision free vehicle dynamics," Ph.D. dissertation, Inst. Transp. Res., Raleigh, NC, USA, 1998.
[32] J. Erdmann, "Lane-changing model in SUMO," in *Proc. SUMO Modeling Mobility Open Data*, vol. 24, May 2014, pp. 77–88.
[33] C. Colberg, B. Tona, W. Stahel, M. Meier, and J. Staehelin, "Comparison of a road traffic emission model (HBEFA) with emissions derived from measurements in the Gubrist road tunnel, Switzerland," *Atmos. Environ.*, vol. 39, no. 26, pp. 4703–4714, Aug. 2005.

YUQING GUO received the B.S. degree from the Harbin Institute of Technology, China, in 2018. She is currently pursuing the Ph.D. degree with the Department of Automation, Tsinghua University, China. Her current research interests include intelligent traffic control, cooperative driving, and optimal control.

HUILE XU received the B.S. degree from Chongqing University, China, in 2016. He is currently pursuing the Ph.D. degree with the Department of Automation, Tsinghua University, China. He is also a visiting Ph.D. Student with the Division of Systems Engineering and Center for Information and Systems Engineering, Boston University, Boston. His research interests include cooperative driving, intelligent vehicles, and optimal control.

YI ZHANG (Member, IEEE) received the B.S. and M.S. degrees from Tsinghua University, China, in 1986 and 1988, respectively, and the Ph.D. degree from the University of Strathclyde, U.K., in 1995. He is currently a Professor of control science and engineering with Tsinghua University. His current research interest includes intelligent transportation systems. His active research areas include intelligent vehicle-infrastructure cooperative systems, analysis of urban transportation systems, urban road network management, traffic data fusion and dissemination, and urban traffic control and management. His research fields also include the advanced control theory and applications, advanced detection and measurement, systems engineering, and so on.

DANYA YAO (Member, IEEE) received the B.S., M.S., and Ph.D. degrees from Tsinghua University, Beijing, China, in 1988, 1990, and 1994, respectively. He is currently a Full Professor with the Department of Automation, Tsinghua University. His research interests include intelligent detection technology, system engineering, mixed traffic flow theory, and intelligent transportation systems.